minerals

MDPI

Article

Scale-Up of Decanter Centrifuges for the Particle Separation and Mechanical Dewatering in the Minerals Processing Industry by Means of a Numerical Process Model

Philipp Menesklou *, Tabea Sinn, Hermann Nirschl and Marco Gleiss

Karlsruhe Institute of Technology (KIT), Institute of Mechanical Process Engineering and Mechanics (MVM), Strasse am Forum 8, 76131 Karlsruhe, Germany; tabea.sinn@kit.edu (T.S.); hermann.nirschl@kit.edu (H.N.); marco.gleiss@kit.edu (M.G.)

* Correspondence: philipp.menesklou@kit.edu; Tel.: +49-721-608-42408

Abstract: Decanter centrifuges are frequently used for thickening, dewatering, classification, or degritting in the mining industry and various other sectors. Their use in an industrial process chain requires a sufficiently accurate prediction of the product and the machine behaviour. For this purpose, experiments on a smaller pilot-scale are carried out for scale-up of a decanter centrifuge, which is usually a major challenge. Predicting the process behaviour of decanter centrifuges from laboratory tests is rather difficult. Basically, there are two common ways of scale-up: First, via analytical methods and the law of similarity, which often requires an enormous experimental effort. Second, using numerical models, which demands a mathematically and physically precise description of the multiple processes running simultaneously in such machines. This article provides an overview of both methods for scale-up of a decanter centrifuge. The concept of a previous developed numerical approach is introduced. Pros and cons of both scale-up methods are compared and further discussed. Experiments on lab-scale, pilot-scale, and industrial-scale decanter centrifuges with two different finely dispersed calcium carbonate water suspensions were carried out and simulations were done to investigate and prove the scale-up capability and transferability of the numerical approach.

Keywords: scale-up; solid-liquid separation; decanter centrifuge; process model; dynamic simulation

Citation: Menesklou, P.; Sinn, T.; Nirschl, H.; Gleiss, M. Scale-Up of Decanter Centrifuges for the Particle Separation and Mechanical Dewatering in the Minerals Processing Industry by Means of a Numerical Process Model. *Minerals* **2021**, *11*, 229. https://doi.org/10.3390/min11020229

Academic Editor: Luis A. Cisternas and Freddy A. Lucay

Received: 1 February 2021
Accepted: 19 February 2021
Published: 23 February 2021

1. Introduction

Solid-liquid separation is an important part of the process chains in many industry sectors, such as the mining industry. For the high throughputs typically expected in such applications, continuously operating decanter centrifuges are a reasonable option. They are frequently used for dewatering and classification of mineral products, such as calcium carbonate water slurries. In general, the scale-up of a decanter centrifuge from pilot to industrial-scale is a major challenge.

Stahl [1] has demonstrated that changing operating parameters often has a contrary effect on the performance of solid-bowl centrifuges. For example, the same separation result can be obtained by various parameter combinations of the process behaviour. This causes the geometry and process conditions to be unable to be simply scaled up linearly. As a result, for a successful scale-up to industrial-scale, experiments on a pilot-scale are required to determine the correct transfer function and hence map the non-linearity of the system. This has the disadvantage that often a significant number of experiments are necessary, which implies a high energy demand, personnel, and cost expenditure.

Research on scale-up for solid-bowl centrifuges has relied primarily on analytical models [2]. Ambler [3–5] introduced the so-called Σ-theory, which is based on the residence time of a particle in the centrifuge assuming a plug-flow, which is related to Stokes' settling velocity. Wakeman and Tarleton [2] presented a very similar approach compared to the Σ-theory. Leung [6] developed a scale-up method considering the flow pattern in a rotating

bowl. All three mentioned analytical methods are introduced in more detail in the next section, and their pros and cons are outlined. At this point, it should be noted that none of the methods mentioned above consider the loading of the centrifuge and its dynamic behaviour during operation, which often leads to significant deviations compared to experimental data.

An increased interest in numerical models has emerged in recent years. On the one hand, there are more detailed, but also computationally time-consuming, computational fluid dynamics (CFD) and discrete element method (DEM) simulations. On the other hand, in dynamic real-time simulations, the computational effort is reduced introducing more assumptions. Therefore, these models require material functions which characterise the real material behaviour in the simulation to compensate the model reduction.

Zhu et al. [7] presented a CFD model for a three-phase decanter centrifuge, which is typically used in oil industry for water/oil/sand separation. The phases were modelled with a Eulerian multiphase approach (so-called particle pseudo-fluid model) in Fluent. Only monodisperse distributed particles are simulated. Sediment build-up, consolidation and transport are not considered. Therefore, the proposed simulation method is not applicable to a decanter centrifuge used for dewatering, or the classification of mineral slurries, where the sediment behaviour plays a major role and polydisperse particle size distributions typically occur. Fernandez and Nirschl [8] proposed a coupled CFD-DEM method for simulating a solid-bowl centrifuge. Firstly, the flow of water and air is calculated with CFD as continuous phases. Secondly, particle movement is modelled with DEM. The method is not directly adaptable to the decanter centrifuge, where additionally a screw rotates with a differential speed and thus induces shear forces to the sediment influencing sediment transport and flow behaviour. Furthermore, Fernandez and Nirschl [8] use particles with a diameter of 125 µm up to 200 µm. Here in this work, finely dispersed products are considered, which means that the particles are typically smaller than 20 µm and the local solids content in a decanter centrifuge often varies between nearly clarified liquid and a densely packed sediment. This would require an extremely high number of very small particles in DEM to map sediment consolidation and transport, which increases the computational effort of the DEM calculation enormously. For this reason, Hammerich et al. [9] developed a multiphase CFD model for application on a tubular centrifuge, which takes sediment consolidation and rheological behaviour into account. The suspension and sediment phase are described using an Euler approach. However, the model is not transferable to the decanter centrifuge in this form, because solver internal algorithms and equations are not adapted to the screw geometry and thus additional shear forces in the sediment caused by the screw are not considered. As previously mentioned, the discussed simulation approaches allow one to predict the physical behaviour of very detailed solid-bowl centrifuges, but are time-consuming and computationally intensive.

For the application in flowsheet and process simulations or model-predictive control algorithms, a significant reduction of the computing time towards real-time simulation is essential. Stiborsky [10] introduced a numerical model to calculate the dewatering of granular products (particles greater 50 µm) in decanter centrifuges. However, the dewatering behaviour of granular products differs substantially from finely dispersed products, meaning that the centrifugal forces are typically no longer sufficient to exceed the capillary forces within the finely dispersed sediment and it remains completely saturated.

Stickland [11] described numerical models for the simulation of batch centrifuges, tubular centrifuges, and the cylindrical part of decanter centrifuges. The author divided the centrifuge into specific sections to calculate settling, sediment consolidation and sediment transport. Stickland [11] obtained the conservation equations of momentum and mass as well as the boundary conditions for the cylindrical part. However, the conical part was neglected, and no equations were formulated for this part. Gleiss et al. [12] provided a dynamic process model considering sediment build-up and classification in the cylindrical part of a counter-current decanter centrifuge, but neglects the cone as well. This conical part of the decanter centrifuge, through which the sediment is transported out of the pool

to the cake discharge, plays indeed a decisive role in the dewatering and transport of the sediment. Therefore, Menesklou et al. [13] extended the numerical model of Gleiss et al. [12] by integrating the conical part of the decanter centrifuge in the model. The work of Menesklou et al. [13] has focused on modelling the conical part, and the results presented in this work are promising but demand further investigations regarding scale-up capability and transferability. So far, the extended material characterisation and validation of this comprehensive approach have only been performed for one finely dispersed mineral product and for one scale.

The aim of this study is to evaluate, in a detailed way, the effectiveness of the simulation method, which includes the transferability of the material characterisation and the scale-up capability. In the present article, the authors highlight and discuss key differences between analytical and numerical scale-up for decanter centrifuges. Simulations are compared to experimental data for a lab-, pilot- and industrial-scale decanter centrifuge based on two different finely dispersed calcium carbonate water slurries (CC1 and CC2) to prove the scale-up capability and transferability of this numerical approach. It is necessary to investigate whether this works with a new calcium carbonate product which behaves differently. This would have the benefit that the simulation method is flexible, particularly in industrial applications, regarding changes in the used product, especially with respect to the transport efficiency of the consolidated sediment, which is calibrated on a lab-scale decanter centrifuge and used for industrial-scale simulations. This leads to the question if this calibration is also valid and sufficient for intermediate scales and therefore an up and down scaling is possible when the transport efficiency is calibrated at one scale, because the residence time behaviour and the centrifugal acceleration can vary significantly between the different sizes.

The next section outlines the analytical scale-up approaches, which are commonly used for the dimensioning of decanter centrifuges. Background information about the material characterisation of the products is provided and limitations of the numerical approach are explained. Next, the calcium carbonate products, centrifuges and experimental procedure are presented. Finally, both scale-up methods are compared and the results are discussed.

2. Analytical Scale-Up Approaches

This section provides an overview of the scale-up of decanter centrifuges by means of analytical equations. The theories have been developed and improved since the 1950s and are widely used in industrial applications [2,6,14]. Decanter centrifuges are continuously working solid-bowl centrifuges. Figure 1 shows a schematic view of the decanter centrifuge with geometric dimensions.

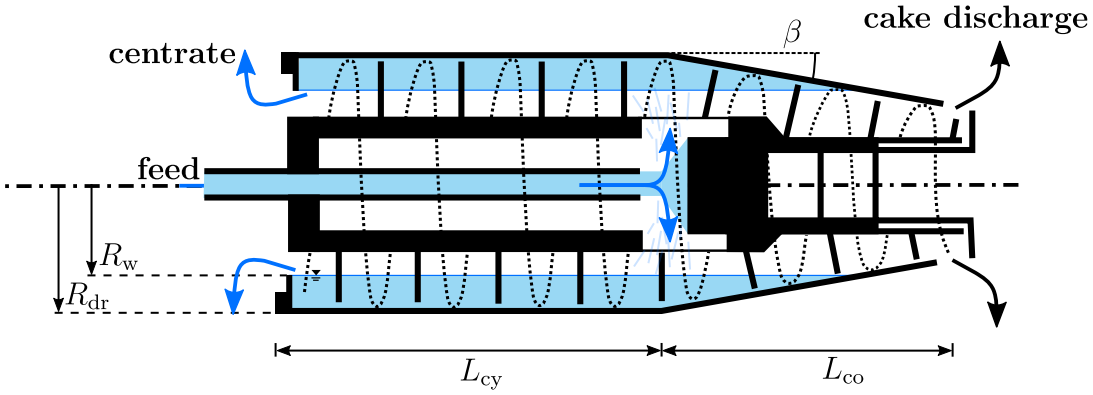

Figure 1. Principle scheme of a counter-current decanter centrifuge with geometrical dimensions.

In general, the feed suspension is accelerated and fed into the pool. The drum rotates with a rotational speed n_{rot}. Due to the centrifugal forces and the density difference between the liquid and solid phase, the particles settle towards the drum wall. The sediment

consolidates and is transported in the direction of the cake discharge as a result of the induced shear forces caused by the screw, which rotates with a small differential speed compared to the bowl of the decanter centrifuge. The clarified liquid is extracted at the centrate outlet. These processes (settling, sediment consolidation, and sediment transport) all take place in the helical screw channel of the decanter centrifuge.

2.1. Σ-Theory

Ambler [3–5] introduces a mathematical approach to compare the settling behaviour between different forms of sedimentation type centrifuges. The so-called Σ-theory is also known as "theory of equivalent area" because the value Σ is the calculated equivalent area of a settling tank theoretically having the same performance in the gravitational field. It is calculated by multiplying the relative centrifugal acceleration C with the characteristic area of apparatus A:

$$\Sigma = CA = C2\pi R_c L_c \tag{1}$$

Here, R_c as the characteristic radius and the characteristic length L_c, have to be defined in a way that includes the geometric specifics of the centrifuge. Often, the mean radius,

$$R_m = \frac{1}{2}(R_w + R_{dr}), \tag{2}$$

is used as characteristic radius. However, the calculation is not standardised. The parameters L_c and R_c are defined differently by various authors and centrifuge companies. This leads to varying results calculating the Σ-values. The difference may easily be a factor of five and may thus entail misleading conclusions. Loll et al. [15] have summarised the different calculation methods and illustrated with an exemplary calculation the previously described differences. The basis of all these approaches is Stokes' settling velocity [16].

$$u_{St} = \frac{4\pi^2}{18}\frac{\Delta\rho}{\eta_l}x_p^2 n_{rot}^2 R_c, \tag{3}$$

adapted to the centrifugal field. Here, $\Delta\rho$ is the density difference between the solid and liquid phase, η_l is the dynamic viscosity of the liquid, x_p is the particle diameter, and n_{rot} is the rotational speed of the drum. The centrifuge throughput is obtained from the residence time of the selected particle with a specific size. This includes Stokes' [16] settling velocity in radial direction and the assumption of plug flow in axial direction towards the centrate, which leads to the following relation:

$$\dot{V} = \frac{4\pi^3}{9}\frac{\Delta\rho}{\eta_l}x_p^2 n_{rot}^2 L_c R_c^2 \tag{4}$$

Now, the scale-up requires a scaling criterion. In the case of classification, the cut particle size x_{cut} has to remain constant in all scales. This means that the same separation efficiency is expected, when the condition

$$\frac{\dot{V}_1}{\dot{V}_2} = \frac{\Sigma_1}{\Sigma_2} = \text{const.} \tag{5}$$

is fulfilled. Leung [6] openly questioned whether Σ-theory is applicable. The author argues that the assumptions are too simplifying and do not cover the decisive physical effects. Firstly, Σ theory is based on Stokes settling. Several studies [17–19] have demonstrated that the settling velocity deviates from Stokes' settling velocity, with increasing solids volume fraction due to the increased momentum exchange between the particles and the continuous liquid phase. Furthermore, the Σ-values correspond to only 50 % recovery instead of 100 %. Therefore, various authors use different calculation definitions, as described above by Loll et al. [15] to adjust the scale-up empirically and compensate for the simplifications. This requires enormous experience and expertise. Moreover, none of these analytical

and empirical approaches consider the fact that solid-bowl centrifuges are filled with a sediment.

2.2. G-Volume Approach

Wakeman and Tarleton [2] introduce a very similar approach compared to Σ-theory. Here, the product of the g-factor C (often named G) and the clarification volume V divided by the volumetric flow rate $\dot{V}$ has to be constant for different scales:

$$\frac{C_1 V_1}{\dot{V}_1} = \frac{C_2 V_2}{\dot{V}_2} = \text{const.} \tag{6}$$

Since this approach is based on the same principles as the Σ-theory, it shows the same limitations as discussed in the previous section. The theory can even be directly converted into the Σ-theory.

2.3. Leung Approach

Leung [6] relates decisive deviations of the Σ theory from the ignored flow pattern. The author assumes that a very thin flow boundary layer exists at the pool surface in a rotating bowl, especially when the fluid surface is free to atmosphere [20]. Below this layer in radial direction, Leung assumes a "stagnant pool". Similar to Σ theory, Leung derives the volumetric flow rate of the clarified overflow $\dot{V}$ as product of Stokes' settling velocity, the surface area of the pool, and the squared acceleration efficiency of the feed ε_a^2:

$$\dot{V} = u_{St} 2\pi R_c L_c \varepsilon_a^2 = \frac{4\pi^3}{9} \frac{\Delta\rho}{\eta_l} x_p^2 n_{rot}^2 L_{cy} R_w^2 \varepsilon_a^2 \tag{7}$$

The characteristic radius R_c is set equal to the weir radius R_w, and the characteristic length L_c is set equal to the length of the cylindrical part L_{cy}. The acceleration efficiency ε_a can be seen as a parameter, which describes the deviation from a perfectly pre-accelerated feed. The cut size x_{cut} determines the maximum particle diameter, which can be separated in the machine. According to Leung [6], the separation criterion is defined as follows:

$$\frac{x_{cut}}{x_c} = \frac{3}{\sqrt{\pi}} \text{Le} \tag{8}$$

x_c is a characteristic particle size (e.g., mean diameter). The Leung number Le is defined as

$$\text{Le} = \sqrt{\frac{\dot{V}\eta_l}{L_{cy}\Delta\rho}} \frac{1}{\omega R_w x_c \varepsilon_a} \tag{9}$$

where ω is the angular velocity. Leung [6] interprets the Leung number as a similarity parameter applicable to the scale-up of clarification, classification, and degritting tasks for solid-bowl centrifuges. The dimensionless number typically should be in a certain range, which is depicted in Table 1.

Table 1. Overview of recommended Leung numbers and applications [6].

Le in -	Size-Cut in µm	Centrifuge Type
0.5 to 5	1 to 10	High-speed small throughput
5 to 20	10 to 45	Medium-speed moderate rate
Above 20	Above 45	Low-speed high throughput

3. Numerical Model and Material Characterisation

This section provides an overview of the used numerical model and the required input parameters. It is intended for use as a stand-alone simulation tool as well as parts of optimisation algorithms and model-predictive control. Therefore, this numerical approach

has the ability to perform simulations in real time, which means that it runs at the same rate or faster than the actual physical process. This advantage is coupled with additional assumptions in the model and a special material characterisation, which is discussed below. These assumptions mean that due to the additionally required computational effort, no detailed flow simulations (like CFD methods) are possible with this approach, which is a limitation. However, flow simulations are not the intention of this simulation tool, but the use as a real time model. Generally, the discretisation in this approach is done along the helical screw channel into compartments, which are linked by mass balances. The settling in each compartment is determined with the separation efficiency, which is obtained by combining the residence time and settling time for each particle class. A uniformly distributed flow in each compartment of the pool is assumed for the residence time behaviour of a particle with specific size. The settling velocity is based on Stokes' settling, which is adapted to the centrifugal field and enhanced by a hindered settling factor. This factor reflects the real settling behaviour at increased solids content compared to Stokes' settling velocity, which is only valid for single particles. It is determined experimentally as a function of the solids volume fraction and explained in more detail below. By solving a differential equation for the compression, the consolidation of the sediment is calculated in each compartment. The properties of the individual compartments can change over time due to sediment build-up or a change in the process parameter and thus reflect the dynamic behaviour of the centrifuge. Further information about the modelling, such as discretisation, numerical algorithms, and governing equations, are explained and discussed in detail in Menesklou et al. [13].

Figure 2 is a graphic summary of the input and output parameters with focus on the material functions.

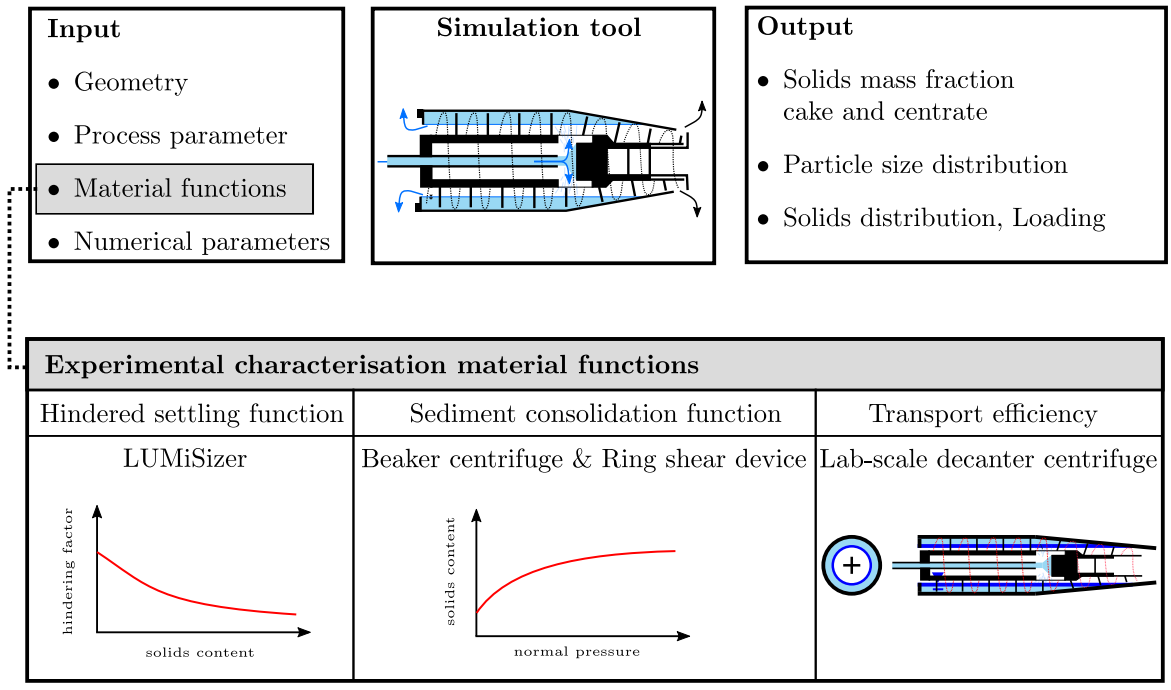

Figure 2. Overview of the required input and calculated output parameters with focus on material functions.

The input parameters can be split into four different categories, as shown in Figure 2. The geometry and process parameters are either given by the centrifuge or set by the operator and are generally available. The numerical parameters are determined by the required spatial and temporal discretisation to ensure a stable simulation. There are numerous mathematical criterions for an appropriate selection. Alternatively, these can be determined by preliminary studies on the influence of discretisation. This means to choose

a sufficiently small time-step and a sufficiently fine spatial discretisation. The material functions specify the real separation behaviour of the processed slurry and thus couple it with shortcut models within the simulation approach. The material functions contain the hindered settling, sediment consolidation, and a transport efficiency of the screw conveyor system. All parameters are determined experimentally using well-established laboratory equipment.

The hindered settling function considers the influence of the solids volume fraction on the settling velocity. Increasing solids' content causes swarm or zone sedimentation, which can accelerate settling compared to Stokes due to cluster formation or can hinder settling due to increased momentum exchange between particles. The settling velocity $u_{\mathrm{set}}(\phi)$ depends on solids volume fraction and is measured with the analytical centrifuge LUMiSizer supplied by LUM GmbH and related to the theoretically expected settling velocity by Stokes u_{St} [21]. Thus, the real settling behaviour is considered in the simulation.

For the hindered settling function $H(\phi)$, a power law approach as used in Michaels and Bolger [22] in the form of

$$H(\phi) = \frac{u_{\mathrm{set}}(\phi)}{u_{\mathrm{St}}} = r_1 \left(1 - \frac{\phi}{r_2}\right)^{r_3} \tag{10}$$

was chosen. The fit parameters are r_1, r_2, and r_3, and are adapted to experimental data. Menesklou et al. [13] show that this function is able to describe the experimentally determined settling behaviour. In Figure 3, the resulting hindered settling functions of the two used calcium carbonate products are plotted against the solids volume fraction.

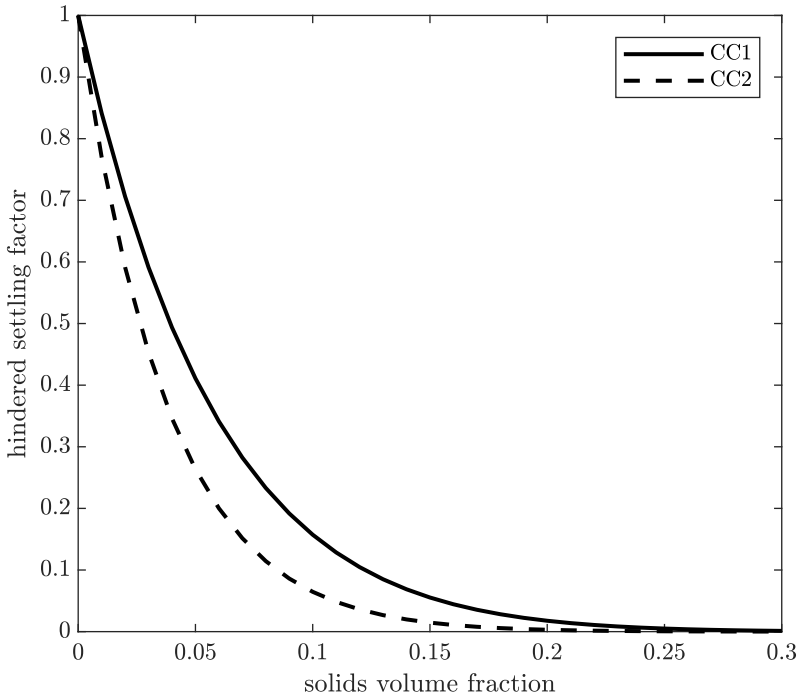

Figure 3. Hindered settling function as a function of the solids volume fraction for the two used calcium carbonate products.

The hindered settling function is $H = 1$ for a solids volume fraction of $\phi \to 0$, where single particle sedimentation according to Stokes can be assumed. The hindered settling factor decreases with increasing solids volume fraction, because of the increasing momentum exchange between the particles.

The sediment of finely dispersed calcium carbonate suspensions, as used in these investigations, shows compressible behaviour. This results in the fact that the solids volume fraction of the sediment is a function of normal stress and varies typically along the height

of the sediment. The compression function introduced by Green et al. [23] with two fit parameters p_1, and p_2,

$$\phi = \phi_{\text{gel}} \left(1 + \frac{p_{\text{y}}}{p_1}\right)^{\frac{1}{p_2}}, \tag{11}$$

describes the correlation between the normal stress p_{y} and the corresponding solids volume fraction ϕ of finely dispersed, compressible sediments. The gel-point ϕ_{gel} is an experimentally determined value which describes the transition between particle settling and sediment consolidation. When shear stress occurs, as caused by the screw of the decanter centrifuge, the sediment can compact additionally [24,25]. Therefore, the uniaxial compression function by Green et al. [23] is adapted and leads to the sediment consolidation function,

$$\phi_{\text{sh}} = K_{\text{p}} \phi_{\text{gel}} \left(1 + \frac{p_{\text{y}}}{p_1}\right)^{\frac{1}{p_2}} + K_{\text{o}}, \tag{12}$$

for the solids volume fraction with additional shear stress ϕ_{sh}. The parameters K_{p}, K_{o}, are empirical parameters which are fitted on the experimental data. If $K_{\text{o}} = 0$ and $K_{\text{p}} = 1$, Equation (12) decreases to uniaxial compression. A detailed description of the measuring procedure can be found in Menesklou et al. [13]. Hammerich et al. [26] present an overview of a modified ring shear cell to measure the yield point of liquid-saturated, compressible sediments. In contrast to Menesklou et al. [13], the consolidation function was extended by the parameter K_{o} to better represent the consolidation function for the complete range. Especially in the region of relatively low normal stress, i.e., in lab-scale, pilot-scale, or even in some industrial-scale decanter centrifuge applications, where centrifugal acceleration is low, the relationship between the sheared and unsheared curve is no longer proportional. Therefore, the parameter K_{o} is introduced to adapt the uniaxial compression curve to the experimental data over the complete range of normal stress.

Figure 4 presents the experimentally determined and fitted sediment consolidation function for the two calcium carbonate-water slurries. The solids volume fraction with shear stress ϕ_{sh} is plotted over the normal stress p_{y}.

The two calcium carbonate products differ in their compression behaviour. The coarser mineral CC1 shows a higher compaction than CC2 at the same normal pressure. This matches with investigations on the compression by Alles and Anlauf [27].

The transport efficiency T is an integral parameter describing the efficiency of the real sediment transport behaviour from the screw towards the cake discharge. The value varies between $T = 0$ and $T = 1$. A transport efficiency of $T = 0$ means that the sediment is not transported along the screw channel. This happens if the sediment is not sufficiently compacted and the shear forces of the screw are not high enough to convey the sediment. A transport efficiency of $T = 1$ corresponds to an ideal sediment transport in axial direction. Experiments have shown that the value for sediments of calcium carbonate water is normally between $T = 0.1$ and $T = 0.9$, due to friction in the sediment and sliding effects between screw and sediment. The transport efficiency is determined experimentally from tests with a lab-scale decanter centrifuge. This leads to the question of whether this transfer is also valid and sufficient for all scales, because the residence time behaviour can vary significantly between the different sizes.

Based on the characterisation of these three material functions for hindered settling, sediment consolidation, and sediment transport, it is possible to perform valid simulations up to the industrial scale. For this purpose, no scaling criteria or further adaptation parameters are necessary, which would be a great advantage and would enable a broad spectrum of simulating and comparing different decanter centrifuges.

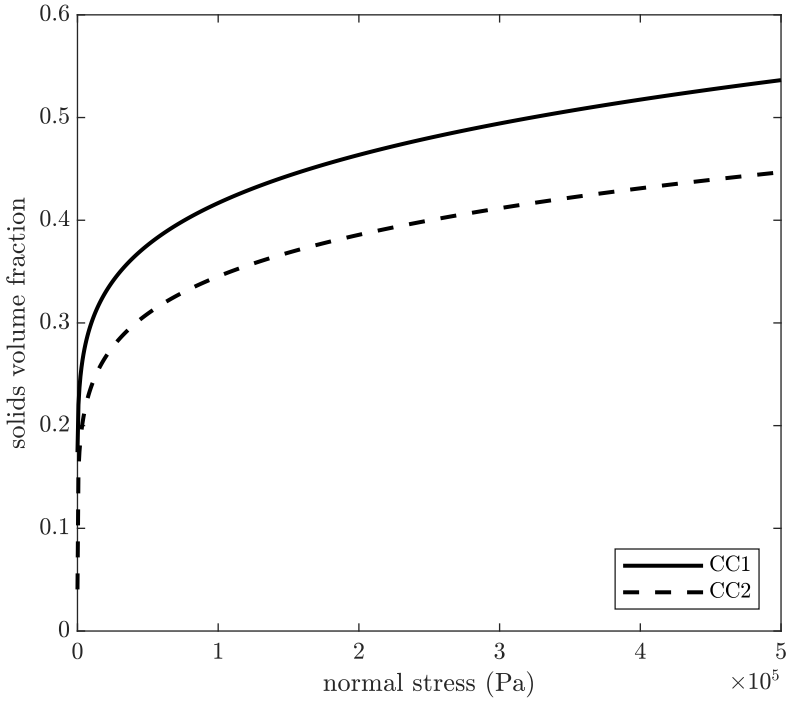

Figure 4. Sediment consolidation function as a function of normal stress for the two used calcium carbonate products.

4. Experimental Setup

Experimental trials were performed for the two presented mineral products on three decanter centrifuges of different sizes. The comparison between experimental data and simulations will be shown in the next section. The intension is to illustrate the accuracy, the scale-up capability, and the transferability of the simulation approach also for other calcium carbonate products. Figure 5 visualises the geometric properties of the apparatuses true to scale.

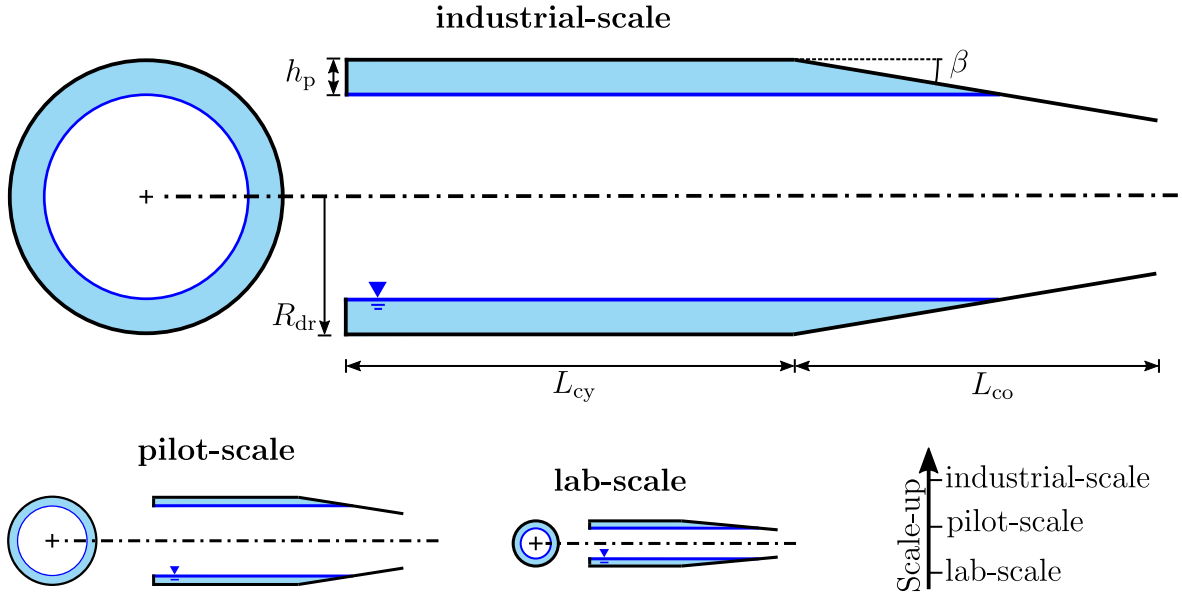

Figure 5. Three sizes of the used decanter centrifuges true to scale.

The three selected decanter centrifuges represent typical sizes. The lab-scale centrifuge is conceived for use in research and high-quality products that are only available in small

quantities. The pilot-scale decanter centrifuge is also frequently used in pilot plants of production sites to check scale-up criteria as an intermediate scale and to carry out basic tests on usability in production. At this point, it should be mentioned that the centrifuges are not exactly geometrically similar in terms of the Buckingham Π theorem. Furthermore, the volumetric flow rates and the solids mass fraction at the inlet are selected to be within the typical application range. The parameters for all three different scales are listed in Table 2.

Table 2. Geometry and process parameters of the decanter centrifuges used.

Parameter	Dimension	Lab-Scale	Pilot-Scale	Industrial-Scale
Length cylinder	m	0.155	0.243	0.746
Length cone	m	0.16	0.174	0.604
Drum radius	m	0.04	0.075	0.229
Cone angle	°	7	10	10
Pool depth	mm	12	14	64
Solids mass fraction inlet CC1	wt.%	9.4	35	35
Solids mass fraction inlet CC2	wt.%	3.4	20.5	18.4
Volumetric flow rate inlet CC1	Lh^{-1}	88	300	2000 to 3000
Volumetric flow rate inlet CC2	Lh^{-1}	33, 54	300	1000 to 2000

To investigate the transferability of the simulation method within the product category of finely dispersed calcium carbonate water suspensions, experiments were carried out on each scale with two different suspensions (CC1 and CC2). Both products show totally different settling (see Figure 3), compression (see Figure 4), and transport behaviour. The particle size was analysed by laser diffraction (Helos/Quixel, Sympatec GmbH, Germany). The logistic function,

$$Q_3(x) = 1 - \frac{1}{1 + \left(\frac{x}{x_{50,3}}\right)^{a_1}}, \tag{13}$$

serves as model function for the distribution function. The parameters $x_{50,3}$ and a_1 were fitted to the measurement results so that the particle size distribution is available as a continuous function and can be discretised initially prior to a simulation. They are specified in Table 3.

Table 3. Fit parameters of particle size distribution for the two calcium carbonate products.

Parameter	Dimension	CC1	CC2
$x_{50,3}$	µm	1.913	1.542
a_1		2.243	2.378

During a series of measurements, the centrifuge was started up, all process parameters set, and then various rotational speeds adjusted. After each variation of rotational speed, the centrifuge was flushed with water to remove deposited sediment. This ensures that previous tests do not influence the current test series. Solids mass fraction of the discharged cake and the centrate was determined gravimetrically. Samples were taken after the machine had reached steady state. Preliminary tests were carried out for each centrifuge to determine how long it takes to reach steady state and thus to determine when samples can be collected after changing the parameters. A time interval of 5 min was determined for the lab- and pilot-scale and 10 min for the industrial-scale. The gravimetric determination of the solids mass fraction of the samples was measured by weighing and drying. Comparing both masses, the average solids mass fraction can be calculated. The sample was weighed in the wet state and again after drying in a drying chamber. To ensure that the sample was completely dry, a minimum drying time was obtained in preliminary tests using the most wet state.

The centrate is released continuously and homogeneously distributed from the centrifuge via a pipeline under the investigated operating conditions. For this purpose, centrate sample was taken directly from this pipe immediately behind the centrate exit. This allows a reliable and representative sampling at this point. The measured value for the solids mass fraction of the cake represents a mean value for the entire discharged sediment layer. Finely dispersed compressible sediments show a distribution of porosity over the sediment height. Typically, the compressed sediment is viscous and pasty, which leads to the fact that the sediment is discharged, rather spread, into an ejection channel. For this reason, a sufficiently large amount of the ejected sediment in the channel is collected at different points to obtain a representative sample. This means that the composition of the collected sample corresponds to the composition of the cake as it would be found immediately before ejection in the centrifuge. Thus, the evaluation of the solids mass fraction of the cake tends to have a higher statistical uncertainty than the centrate due to the sampling. In the diagrams in the following section, no error bars are plotted. The measurements are single measurements and are intended to validate the simulations.

5. Results and Discussion

In this section, simulations are compared to experimental data to discuss the scale-up capability and transferability of this numerical approach. Advantages and disadvantages of both scale-up methods are highlighted and discussed.

Figure 6 shows the solids mass fraction of the cake as a function of the rotational speed. Simulations were done for all three scales for CC1 and were compared to experimental values.

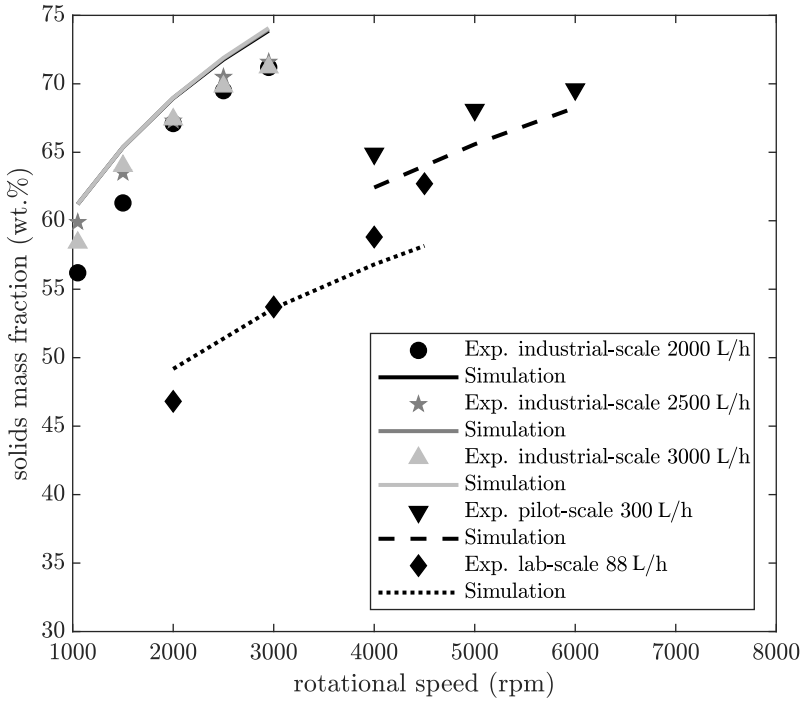

Figure 6. Solids mass fraction of the cake for three decanter centrifuge scales, volumetric flow rates, and rotational speeds: Comparison of simulation and experiment for CC1.

For both simulation and experimental data, the solids mass fraction increases to higher rotational speeds for each scale, which is explainable by the rising centrifugal acceleration. The relative deviation between simulation and experiment is always smaller than 10 wt.%. This is within the range of the expected accuracy of such a process model. Furthermore, it should be mentioned here that the transport of solids requires a three-dimensional description, but the model uses a simplified two-dimensional description, which can

reduce the prediction accuracy. The solids mass fraction in the cake varies significantly for different scales for a specific rotational speed. This is because the drum radius is proportional to the centrifugal acceleration and the height of the sediment has an influence on the compression. The drum radius for the lab-scale machine is substantially smaller (see Table 2) than that of an industrial-scale machine. Therefore, a much smaller centrifugal acceleration is reached. Additionally, the throughput of an industrial-scale centrifuge is basically much higher, and the pool is, in principle, deeper. As a result, a higher sediment builds up in the pool, which causes higher centrifugal pressure on the sediment and thus leads to a more compacted cake. The variation of the volumetric flow rate has practically no significant influence on the solids mass fraction in the cake for the simulation of the industrial-scale decanter centrifuge. The same behaviour is observed for the experimental data. This provides preliminary evidence that the simulation can predict the influence of the volumetric flow rate on the solids content of the cake.

Figure 7 shows the solids mass fraction of the centrate corresponding to data from Figure 6.

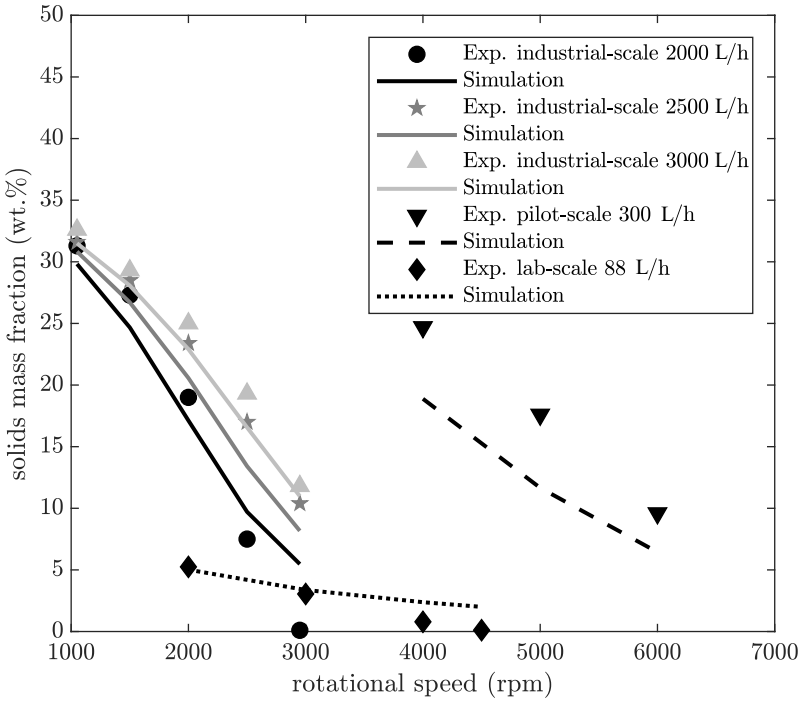

Figure 7. Solids mass fraction of the centrate for three decanter centrifuge scales, volumetric flow rates, and rotational speeds: Comparison of simulation and experiment for CC1.

The solids mass fraction of the centrate decreases with increasing rotational speed. In general, the simulation results here also show a good agreement with experimental data. The simulation results of the pilot-scale machine are smaller than the experimental results. A possible reason for this discrepancy might be that the machine was almost fully loaded by measuring the solids content with this parameter combination during the test series. This may have resulted in a partial resuspension of already separated particles, as Stahl and Langeloh [28] have previously shown. This effect is currently not considered in the simulation and possibly causes this difference.

In analogy to the two previous figures, simulations are compared with experimental data for the product CC2. In Figure 8, the solids mass fraction of the cake is plotted for material CC2 for different scales.

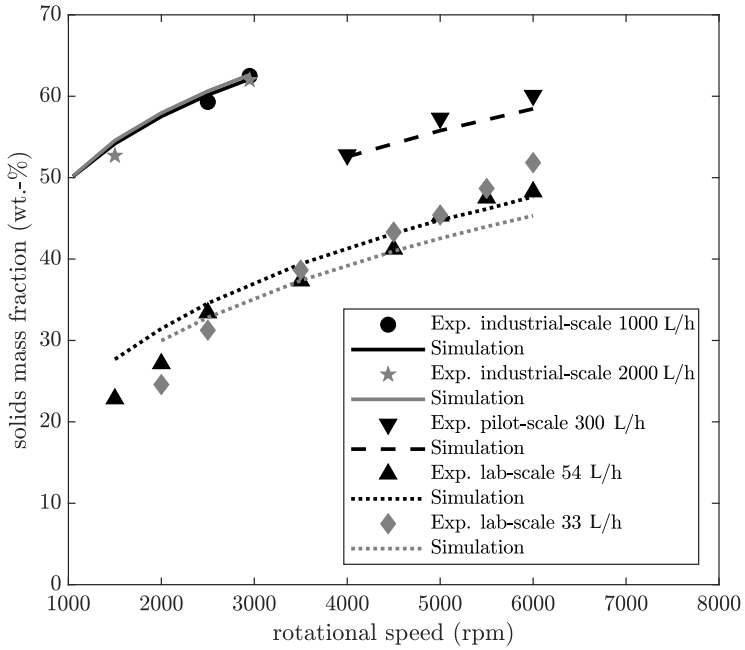

Figure 8. Solids mass fraction of the cake for three decanter centrifuge scales, volumetric flow rates, and rotational speeds: Comparison of simulation and experiment for CC2.

Similar dependencies of the solids mass fraction on the rotational speed are observed, as shown in Figure 6. The simulation results show a relative deviation of less than 10 wt.% compared to the experimental data, except for the lab-scale data at 33 Lh^{-1} for 1500 rpm, 2000 rpm, and 6000 rpm. However, the absolute deviation of these points is less than 5 wt.%. This is still within the experimental measurement tolerance. Furthermore, it should be underlined that all three centrifuges, representing different scales, can be simulated with appropriate accuracy only on the basis of the material characterisation described previously.

Figure 9 illustrates that the solids mass fraction of the centrate is dependent on the rotational speed in analogy to Figure 7 and corresponding to data from Figure 8.

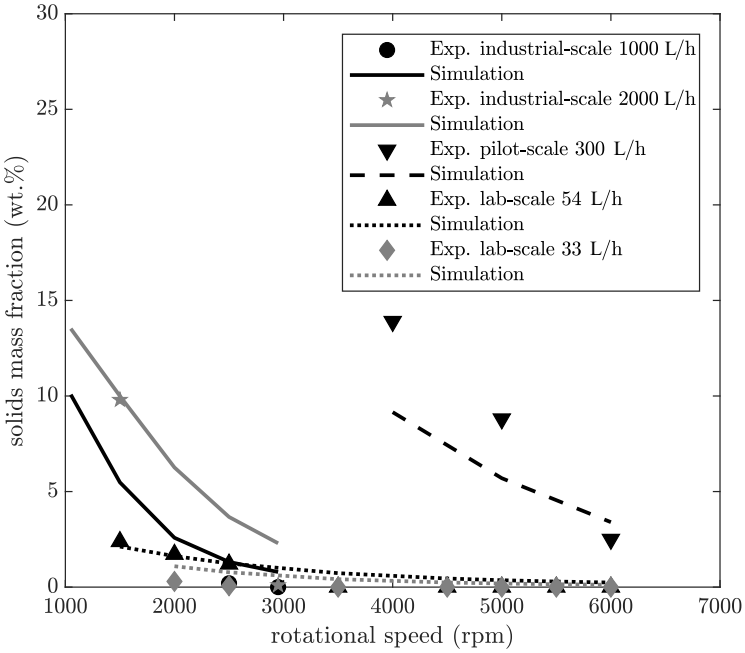

Figure 9. Solids mass fraction of the centrate for three decanter centrifuge scales, volumetric flow rates, and rotational speeds: Comparison of simulation and experiment for CC2.

As previously discussed, the solids content in the centrifuge decreases with increasing rotational speed for both experimental data and simulation. In principle, the results agree well with each other and the absolute deviation is less than 5 wt.%. Furthermore, the physical behaviour of the simulation is reasonable. This indicates that the simulation approach can be applied to further finely dispersed mineral products.

Figure 10 illustrates an exemplary scale-up with the Σ-theory and the numerical model. Therefore, separation efficiency is plotted over rotational speed. The separation efficiency is defined as the ratio of solids mass that has been removed from the feed stream in the centrifuge to the initial solids mass at the feed.

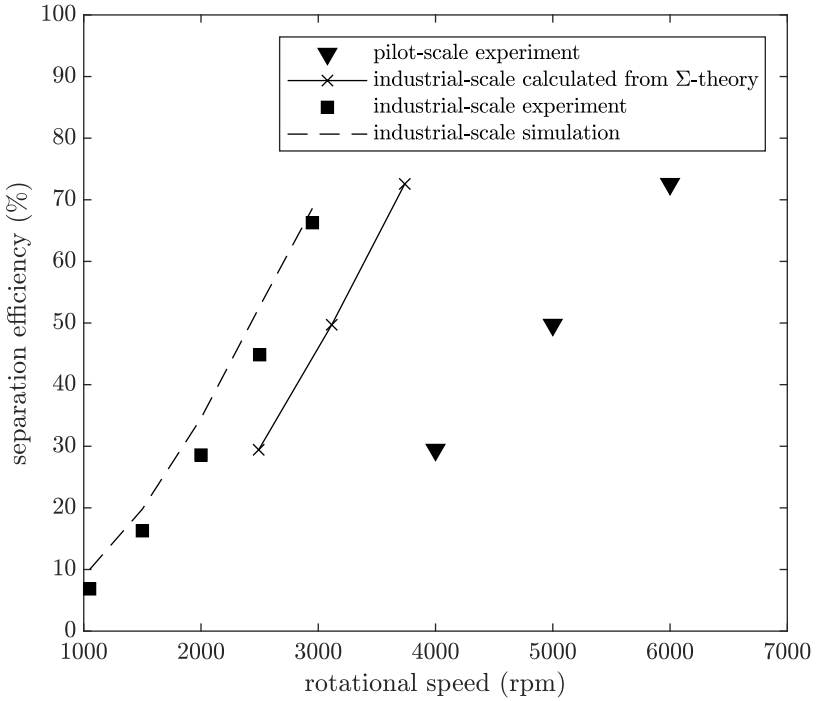

Figure 10. Comparison of scale-up via Σ-theory, and simulation from pilot-scale to industrial-scale for CC1.

This example represents a typical scale-up problem. The dimensioning of an industrial-scale centrifuge is to be determined based on pilot-scale trials. Firstly, pilot-scale tests are done at a volumetric flow rate of 300 Lh^{-1}. The corresponding Σ-values are calculated from the geometry of the machine and the selected centrifugal acceleration according to Equation (1). This allows the scaling criterion (ratio of throughput to Σ-value, see Equation (5)) to be obtained for each experimentally measured parameter combination. The volumetric flow rate in this example is set to 3000 Lh^{-1} for the industrial-scale decanter centrifuge. By considering the scaling criterion, the corresponding Σ-values of the industrial-scale decanter centrifuge can be calculated. It follows from these corresponding Σ-values that, on the one hand, the optimal geometry (characteristic radius and length) or, on the other hand, the optimal centrifugal acceleration and thus rotational speed can be obtained. In this case, the geometry of the industrial-scale machine is defined. Therefore, the resulting rotational speeds required for the industrial-scale apparatus are calculated. The result of the Σ-theory does not coincide with the experimental results of the industrial-scale decanter centrifuge. Σ theory leads to higher rotational speeds than observed in the experiment, which normally means higher energy consumption. The simulation method shows very good agreement with the experimental results, as already discussed previously in this section, and provides sufficient results for scale-up. As a consequence, Σ theory would need an empirical correction parameter to predict the correct machine behaviour in this case.

The material functions, which serve as input parameters for the simulation, are determined for a specific product with discontinuous analytical centrifuges on the laboratory scale. Only the transport efficiency, which describes the deviation from ideal transport behaviour, has to be determined by experiments on a laboratory decanter centrifuge. However, Menesklou et al. [13] have shown that the influence of this variable has a minor influence on the result in investigated industrial-scale applications. This demonstrates that a scale-up of decanter centrifuges from a laboratory scale is possible using the presented numerical approach.

The scale-up of the solids mass fraction in the cake is not possible with the analytical methods presented. These approaches do not consider dewatering and transport models of the sediment within the centrifuge and therefore cannot provide a prediction of the solids mass fraction of the cake. Contrary to this, a model for the dewatering and transport of finely dispersed suspensions is implemented in the numerical approach. Hence, the material behaviour of the sediment within the complete centrifuge can be investigated. Furthermore, due to the discretisation of the apparatus, parameters such as particle size distribution, solids content, etc. can be determined locally and in a time-resolved manner in the centrifuge. These parameters are otherwise not measurable or only with high experimental effort in the apparatus. The analytical method only provides integral parameters of the decanter centrifuge.

To demonstrate this additional feature of the numerical approach, an example is discussed. The industrial-scale centrifuge with product CC1 at a feed rate of 3000 Lh^{-1} is selected. Figure 11 illustrates the solids mass fraction of the suspension along the helical screw path of the centrifuge. The relative length of the decanter L_{rel} centrifuge describes the relative position in the cylindrical part of the decanter centrifuge. The feed enters the apparatus at the transition point between the conical and cylindrical parts, which corresponds to $L_{\mathrm{rel}} = 0$. The centrate is drawn-off at $L_{\mathrm{rel}} = 1$.

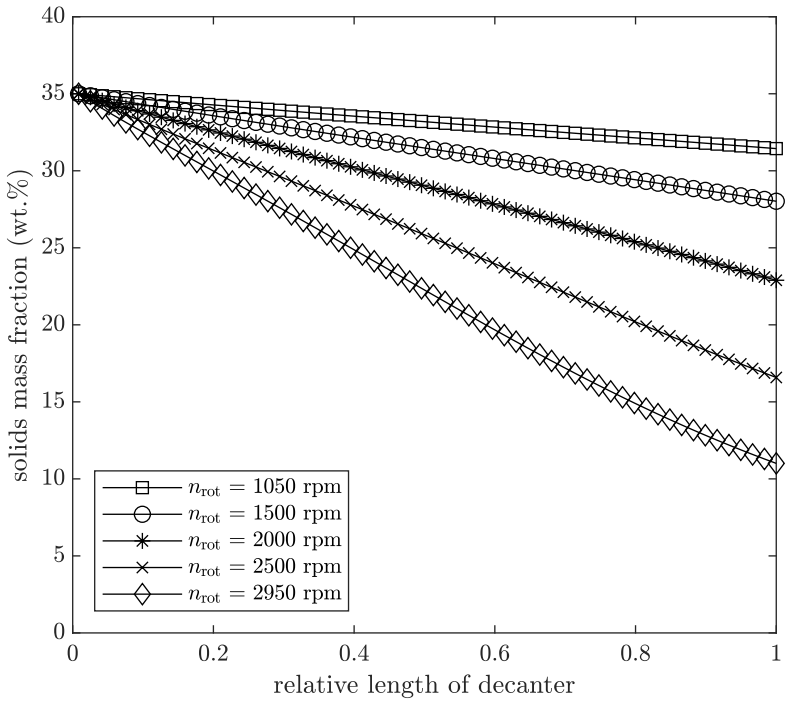

Figure 11. Solids mass fraction along unrolled helix for industrial-scale decanter centrifuge with CC1 for different rotational speeds at a feed rate of 3000 Lh^{-1}.

The solids mass fraction of the suspension decreases approximately linearly in the cylindrical part. This shows that the entire length of the centrifuge is used for separation and the separation is evenly distributed. Figure 12 shows the particle size distributions

of the feed and centrate and along the relative length of the centrifuge as cumulative sum distribution.

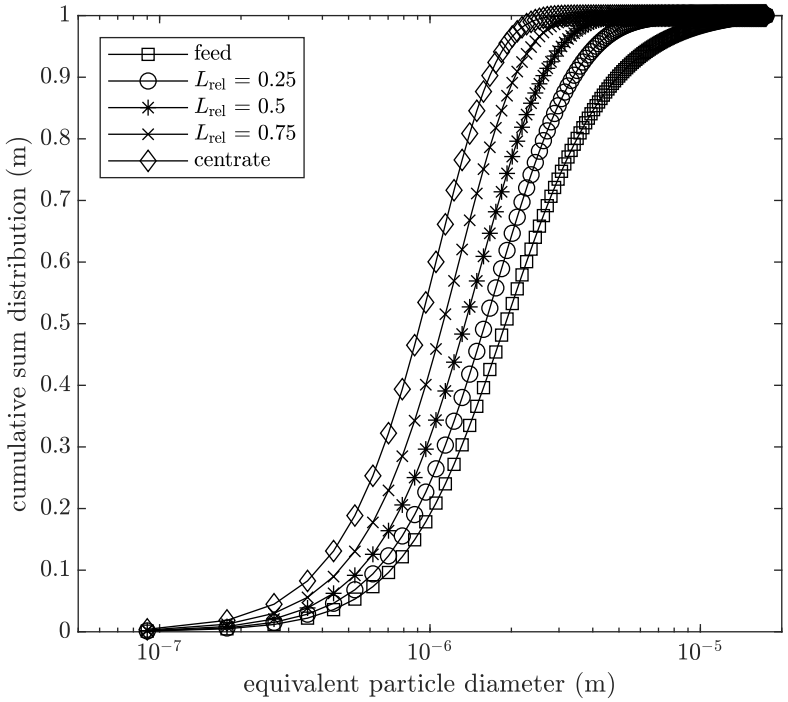

Figure 12. Particle size distribution along unrolled helix for industrial-scale decanter centrifuge with CC1 at a rotational speed of 2950 rpm and a feed rate of 3000 Lh^{-1}.

Generally, the particle size distribution changes from feed to centrate to smaller particle size classes. Furthermore, it should be mentioned that the slope of the distribution changes along the centrifuge length. On the first 25% of the length of the centrifuge, rather bigger particles are deposited. After that, smaller particle size classes are separated. This can be derived from the theory. Stokes' settling velocity is proportional to the square of the particle diameter. It follows that if all particles have the same residence time in the apparatus, smaller particles are separated later. Especially for the classification, it is helpful to know where the separation of the individual size classes takes place. With an analytical scale-up approach, this cannot be determined at this level of detail.

6. Conclusions

Firstly, this article provides an overview of the concepts of three analytical scale-up approaches for decanter centrifuges. The advantages and disadvantages regarding the limits of applicability are discussed. Secondly, simulations, which were performed with a simulation tool as introduced in Menesklou et al. [13], are compared to experimental data for three different scales of decanter centrifuges and two different products. The data provide convincing evidence demonstrating the scale-up capability and transferability to other products of this numerical method. The development of numerical methods and modelling of centrifuges in general and of decanter centrifuges in particular is often complex and time intensive. However, if successfully validated, they are powerful tools. With this simulation tool, various sizes from laboratory to industrial scale can be simulated comprehensively. In addition, parameters that are not optically and spatially accessible during the operation of the machine can be observed locally and in a time-resolved manner as a result of the discretisation. Furthermore, it can also be integrated into optimisation algorithms. This enables determining an ideal geometry and ideal process parameters for the required product. Contrary to this, the analytical methods are mathematically simpler. The computational effort is negligible compared to the numerical methods. Therefore, many

simplifications of the system are necessary, which can result in significant discrepancies with respect to the machine's real behaviour.

The next step is to integrate the developed and validated model into optimisation algorithms and to test them with focus on classification, dewatering, and degritting applications. Two basic aspects are to be optimised. On the one hand, the optimisation algorithm for a defined centrifuge should derive the optimal process parameters for a product, which finally results in a model predictive control. On the other hand, it should find the best possible option from a given selection of machines according to given parameters. If necessary, effects that have not been considered so far will have to be integrated into the numerical simulation tool in the future. Here, it has the potential to integrate the existing model into a so-called grey box model. This links analytical and numerical models with a neural network, which learns to predict deviations by comparing simulation data with experimental data and thus to include non-modelled effects with known physical relationships.

Author Contributions: Conceptualization, P.M.; Formal analysis, P.M.; Investigation, P.M.; Methodology, P.M.; Project administration, P.M.; Software, P.M.; Supervision, H.N. and M.G.; Validation, P.M.; Visualization, P.M.; Writing—original draft, P.M.; Writing—review and editing, T.S. All authors have read and agreed to the published version of the manuscript.

Funding: This research received no external funding.

Institutional Review Board Statement: Not applicable.

Informed Consent Statement: Not applicable.

Data Availability Statement: Not applicable.

Acknowledgments: We acknowledge support by the KIT-Publication Fund of the Karlsruhe Institute of Technology.

Conflicts of Interest: The authors declare no conflict of interest.

Abbreviations

The following abbreviations are used in this manuscript:

CFD	Computational Fluid Dynamics
DEM	Discrete Element Method

References

1. Stahl, W.H. *Fest-Flüssig-Trennung. 2, Industrie-Zentrifugen. Maschinen-& Verfahrenstechnik*; DrM Press: Maennedorf, Switzerland, 2004.
2. Wakeman, R.J.; Tarleton, S. *Solid/liquid Separation: Scale-Up of Industrial Equipment*, 1st ed.; Elsevier: Oxford, UK, 2005; OCLC: 254305213.
3. Ambler, C.M. The theory of scaling up laboratory data for the sedimentation type centrifuge. *J. Biochem. Microbiol. Technol. Eng.* **1959**, *1*, 185–205. [CrossRef]
4. Ambler, C. The evaluation of centrifuge performance. *Chem. Eng. Prog.* **1952**, *48*, 150–158.
5. Ambler, C. Theory of centrifugation. *Ind. Eng. Chem.* **1961**, *53*, 430–433. [CrossRef]
6. Leung, W.W.F. *Industrial Centrifugation Technology*; McGraw-Hill: New York, NY, USA, 1998.
7. Zhu, M.; Hu, D.; Xu, Y.; Zhao, S. Design and computational fluid dynamics analysis of a three-phase decanter centrifuge for oil-water-solid separation. *Chem. Eng. Technol.* **2020**, *43*, 1005–1015. [CrossRef]
8. Romaní Fernández, X.; Nirschl, H. Simulation of particles and sediment behaviour in centrifugal field by coupling CFD and DEM. *Chem. Eng. Sci.* **2013**, *94*, 7–19. [CrossRef]
9. Hammerich, S.; Gleiss, M.; Stickland, A.D.; Nirschl, H. A computationally-efficient method for modelling the transient consolidation behavior of saturated compressive particulate networks. *Sep. Purif. Technol.* **2019**, *220*, 222–230. [CrossRef]
10. Stiborsky, M. *Numerische Simulation der Entfeuchtung Körniger Feststoffe in Dekantierzentrifugen*; Berichte aus der Verfahrenstechnik, Shaker: Aachen, Germany, 2004; OCLC: 76643773.
11. Stickland, A.D. Solid-Liquid Separation in the Water and Wastewater Industries. Ph.D. Thesis, University of Melbourne, Melbourne, Australia, 2005.
12. Gleiss, M.; Hammerich, S.; Kespe, M.; Nirschl, H. Development of a dynamic process model for the mechanical fluid separation in decanter centrifuges. *Chem. Eng. Technol.* **2018**, *41*, 19–26. [CrossRef]

13. Menesklou, P.; Nirschl, H.; Gleiss, M. Dewatering of finely dispersed calcium carbonate-water slurries in decanter centrifuges: About modelling of a dynamic simulation tool. *Sep. Purif. Technol.* **2020**, *251*, 117287. [CrossRef]
14. Records, A.; Sutherland, K. *Decanter Centrifuge Handbook*; Elsevier: Oxford, UK, 2001. [CrossRef]
15. Loll, U.; Thomé-Kozmiensky, K.J.; Recycling-Congress, I. (Eds.) *Recycling von Klärschlamm. 3: Klärschlammaufbereitung und-Behandlung*; Technik, Wirtschaft, Umweltschutz; EF-Verlag für Energie- und Umwelttechnik GmbH: Berlin, Germany, 1992; OCLC: 75352531.
16. Stokes, G.G. *Mathematical and Physical Papers*; Cambridge University Press: Cambridge, UK, 2009. [CrossRef]
17. Buscall, R.; Goodwin, J.; Ottewill, R.; Tadros, T. The settling of particles through Newtonian and non-Newtonian media. *J. Colloid Interface Sci.* **1982**, *85*, 78–86. [CrossRef]
18. Ekdawi, N.; Hunter, R.J. Sedimentation of disperse and coagulated suspensions at high particle concentrations. *Colloids Surf.* **1985**, *15*, 147–159. [CrossRef]
19. Richardson, J.F.; Zaki, W.N. The sedimentation of a suspension of uniform spheres under conditions of viscous flow. *Chem. Eng. Sci.* **1954**, *3*, 65–73. [CrossRef]
20. Leung, W.W.F. Inferring in-situ floc size, predicting solids recovery, and scaling-up using the Leung number in separating flocculated suspension in decanter centrifuges. *Sep. Purif. Technol.* **2016**, *171*, 69–79. [CrossRef]
21. Lerche, D. Dispersion stability and particle characterization by sedimentation kinetics in a centrifugal field. *J. Dispers. Sci. Technol.* **2002**, *23*, 699–709. [CrossRef]
22. Michaels, A.S.; Bolger, J.C. Settling Rates and Sediment Volumes of Flocculated Kaolin Suspensions. *Ind. Eng. Chem. Fundam.* **1962**, *1*, 24–33. [CrossRef]
23. Green, M.D.; Eberl, M.; Landman, K.A. Compressive yield stress of flocculated suspensions: Determination via experiment. *AIChE J.* **1996**, *42*, 2308–2318. [CrossRef]
24. Erk, A. Rheologische Eigenschaften Feindisperser Suspensionen in Filtern und Zentrifugen. Ph.D. Thesis, Universität Karlsruhe (TH), Karlsruhe, Germany, 2006.
25. Channell, G.M.; Zukoski, C.F. Shear and compressive rheology of aggregated alumina suspensions. *AIChE J.* **1997**, *43*, 1700–1708. [CrossRef]
26. Hammerich, S.; Stickland, A.D.; Radel, B.; Gleiss, M.; Nirschl, H. Modified shear cell for characterization of the rheological behavior of particulate networks under compression. *Particuology* **2020**, *51*, 1–9. [CrossRef]
27. Alles, C.; Anlauf, H. Filtration mit kompressiblen Kuchen: Effiziente Konzeptefür eine anspruchsvolle Trennaufgabe. *Chem. Ing. Tech.* **2003**, *75*, 1221–1230. [CrossRef]
28. Stahl, W.; Langeloh, T. Improvement of clarification in decanting centrifuges. *Chem. Ing. Tech.* **1983**, *55*, 324–325. [CrossRef]